Instabilities and self-oscillations in atomic four-wave mixing

J. Heurich, H. Pu, M. G. Moore, and P. Meystre
Optical Sciences Center, University of Arizona, Tucson, Arizona 85721

(Received 26 May 2000; published 8 February 2001)

The development of integrated, waveguide-based atom optical devices requires a thorough understanding of nonlinear matter-wave mixing processes in confined geometries. This paper analyzes the stability of counterpropagating two-component Bose-Einstein condensates in such a geometry. The steady-state field equations of this system are solved analytically, predicting a multivalued relation between the input and output field intensities. The spatiotemporal linear stability of these solutions is investigated numerically, leading to the prediction of a self-oscillation threshold that can be expressed in terms of a matter-wave analog of the Fresnel number in optics.

DOI: 10.1103/PhysRevA.63.033605 PACS number(s): 03.75.Be, 03.75.Fi, 42.65.Pc

I. INTRODUCTION

The recent development of narrow atomic microfabricated waveguides [1–7] has raised the exciting possibility of the design and manufacture of integrated atom-interferometry-based sensing devices. With the inclusion of an ''atom laser'' [8–11] as a high-brightness source of coherent atomic matter waves, it is possible to imagine ''practical'' devices, which could compete with or out perform conventional optical interferometric sensors. The use of high-density atomic fields comes at a price, however, as atomic matter waves are subject to nonlinear wave mixing due to atom-atom interactions. It is of crucial importance, therefore, to understand the effects of nonlinear wave mixing on wave-guide based atom-optics devices so that they may eventually be controlled or even exploited. In this spirit, the present paper is a first attempt at an analysis of wave-mixing instabilities in quasi-one-dimensional ultracold atomic samples.

The observation of atomic four-wave mixing [12–18] and solitons [19–25] in Bose-Einstein condensates of dilute atomic vapors [26–28] clearly demonstrate both the significance of nonlinear effects in quantum degenerate atomic fields, as well as the benefits of exploiting the mathematical analogy between the nonlinear equations describing self-interacting Schrödinger fields and those describing the propagation of light in nonlinear media. Nonlinear wave-mixing instabilities have been studied extensively in nonlinear optics, and many of the techniques and results developed here can readily be adapted to the problem at hand.

Focusing on effective one-dimensional geometries, the question of stable and unstable steady-state configurations has long been a topic of optical research. Winful and Marburger [29] first proposed that bistability could occur in collinear degenerate four-wave mixing and shortly thereafter Silberberg and Bar-Joseph [30] showed that even for the rather simple case of equally polarized counterpropagating laser beams, instabilities and even chaos may occur in the dynamical behavior. Multibranched steady-state solutions were first derived by Kaplan and Law [31], however the stability of the steady-state field configurations were not determined. Considerable work on the spatial or temporal stability of such systems was subsequently carried out by many others [32–37]. In particular, optical instabilities and polarization bistability were experimentally observed in sodium vapor [38,39].

Bistability and nonlinear instability are typically related to four-wave-mixing phenomena in systems that exhibit a cubic nonlinearity. In ultracold atomic systems it is readily shown that in the *s*-wave scattering approximation the form of the self-interaction is that of a cubic nonlinearity. A recent paper by Law and co-workers [40] analyzed four-wave-mixing processes between the hyperfine ground-state components of components of a ^{23}Na spinor condensate confined in an optical dipole trap. Goldstein and Meystre [41] presented a full quantum-mechanical theory of four-wave mixing in a system where two $m_F=0$ momentum side modes were counterpropagating while the $m_F=\pm 1$ states were at rest.

In the present paper we investigate a collinear four-wave-mixing geometry as sketched in Fig. 1, where each of the counterpropagating matter waves can be in one of two different atomic states, for example two hyperfine state levels of ^{87}Rb. This situation is closely analogous to the optical case, the two internal atomic states taking the place of the polarizations of the field. As such, this system is formally equivalent to the case of counterpropagating light fields in an Kerr medium.

In contrast to the exact quantum treatment of Refs. [40] and [41], our analysis is based on a mean-field approach, the matter-wave equivalent of treating the electromagnetic field classically. We investigate both the steady-state and dynamical behavior of the system by a combination of analytical and numerical methods. The output fields are found to generally exhibit a multivalued dependence on the inputs, characteristic of bistable and multistable systems. The stability analysis for this particular configuration, however, shows that only the upper branch of the steady-state curve is stable against small perturbations. More interesting is the occurrence of a threshold behavior in the output fields indicating the onset of self-oscillations in the system. The feedback mechanism leading to this effect is the grating established in the medium by the interference between the various fields.

We note that matter-wave bistability was recently predicted in a simple model of a driven nonlinear Gross-Pitaevskii equation [42], which neglected, however, the effects of collisions between the strong driving field and the condensate. In contrast, the present system includes both the

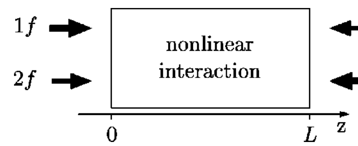

FIG. 1. Four matter waves incident into a region of nonlinear interaction. The two forward moving and the two backward propagating modes, with opposite wave vectors, are distinguished by their internal state.

effect of two-body collisions, and fully accounts for propagation effects.

This paper is organized as follows: Section II introduces our model and derives the nonlinear partial differential equations describing the propagation of the interacting atomic beams. Section III solves these equations analytically in steady state and shows the appearance of multistable solutions and threshold behavior. The stability of the steady-state solutions is investigated in Sec. IV using numerical methods, while Sec. V discusses the onset of self-oscillations. Finally, Sec. VI is a summary and conclusion.

II. MODEL

We consider an ultracold two-component Schrödinger field $\hat{\mathbf{\Psi}}(\mathbf{r},t)=[\hat{\Psi}_1(\mathbf{r},t),\hat{\Psi}_2(\mathbf{r},t)]^T$, the indices 1 and 2 labeling the internal state of the atoms of mass m, e.g., two hyperfine ground states. These fields consist of two counterpropagating plane waves that interact propagating along the z axis in an interaction region $0\leqslant z\leqslant L$, the nonlinear interaction outside this region being turned off, e.g., by tuning a magnetic field to a Feshbach resonance.

Our starting point for the description of this system is the many-body Hamiltonian describing the evolution of a two-component condensate, the effects of collisions being described in the s-wave scattering approximation,

$$\begin{aligned}\mathcal{H}=&\sum_{j=1,2}\int d^3r\hat{\Psi}_j^\dagger(\mathbf{r},t)\left(\frac{\hat{p}^2}{2m}+V_j\right)\hat{\Psi}_j(\mathbf{r},t)\\&+\frac{\hbar}{2}\int d^3r(g_1\hat{\Psi}_1^\dagger\hat{\Psi}_1^\dagger\hat{\Psi}_1\hat{\Psi}_1+g_2\hat{\Psi}_2^\dagger\hat{\Psi}_2^\dagger\hat{\Psi}_2\hat{\Psi}_2\\&+2g_x\hat{\Psi}_1^\dagger\hat{\Psi}_2^\dagger\hat{\Psi}_1\hat{\Psi}_2),\end{aligned}\tag{1}$$

where the scattering strengths g_i are related to their respective s-wave scattering lengths a_i by

$$g_i=\frac{4\pi\hbar a_i}{m}.\tag{2}$$

For $T\rightarrow 0$, the condensate is well described by a two-component Hartree condensate wave function $\Phi(\mathbf{r},t)=[\Phi_1(\mathbf{r},t),\Phi_2(\mathbf{r},t)]^T$, governed by the coupled Gross-Pitaevskii nonlinear Schrödinger equations

$$i\hbar\dot{\Phi}_1=\left(\frac{\hbar^2}{2m}\nabla^2+V_1\right)\Phi_1+\hbar N[g_s|\Phi_1|^2+g_x|\Phi_2|^2]\Phi_1,\tag{3}$$

and similarly for Φ_2 with $1\leftrightarrow 2$, where the total atomic density is normalized to 1 by factoring out the number of atoms N. Quantum fluctuations about this solution can be analyzed by introducing the mean-field approximation

$$\hat{\Psi}_i(\mathbf{r},t)\simeq\Phi_i(\mathbf{r},t)+\delta\hat{\psi}_i(\mathbf{r},t),\tag{4}$$

where the bosonic operator $\delta\hat{\psi}_i(\mathbf{r},t)$ describes small fluctuations about the mean field $\Phi_i(\mathbf{r},t)=\langle\hat{\Psi}_i(\mathbf{r},t)\rangle$. This analysis will be the subject of future work.

We assume that the atomic fields are tightly confined in the transverse dimension but free to move in the third one such that the motional degrees of freedom in the $x-y$ plane are frozen, a situation that could be realized in atomic waveguides. In that case, we may factorize the ground-state Hartree wave function into a parallel and a transverse part as

$$\Phi_j(\mathbf{r},t)=\phi_\perp^{(j)}(x,y)\phi_j(z,t)e^{-i\omega_j t},\tag{5}$$

where $\phi_\perp^{(j)}(x,y)$ is taken to be the normalized ground state of the transverse potential $V_j(x,y)$ with energy $\hbar\omega_j$. The problem is then reduced to an effective one-dimensional geometry, with the longitudinal condensate wave function satisfying the one-dimensional nonlinear Schrödinger equation

$$\begin{aligned}i\hbar\dot{\phi}_1(z,t)=&-\frac{\hbar^2}{2m}\frac{\partial^2}{\partial z^2}\phi_1(z,t)+\hbar N[\eta_1 g_1|\phi_1(z,t)|^2\\&+\eta_x g_x|\phi_2(z,t)|^2]\phi_1(z,t)\end{aligned}\tag{6}$$

and similarly for $\phi_2(z)$ with $1\leftrightarrow 2$. Here

$$\eta_j=\int dx\,dy\,|\phi_\perp^{(j)}|^4,\quad j=1,2$$

$$\eta_x=\int dx\,dy|\phi_\perp^{(1)}|^2|\phi_\perp^{(2)}|^2.\tag{7}$$

We consider the situation where two counterpropagating beams of matter waves are moving along the axis of the waveguide, with

$$\phi_j(z,t)=[\phi_{jf}(z,t)e^{ikz}+\phi_{jb}(z,t)e^{-ikz}]e^{-i\omega t},\tag{8}$$

where $j=1,2$, the subscripts f and b stand for forward- and backward-propagating waves, and $\hbar k^2/2m=\omega$. We assume that the spatial envelopes of these beams vary slowly over a de Broglie wavelength, the atom optics version of the slowly varying envelope approximation,

$$\left|\frac{\partial^2}{\partial z^2}\phi_m\right|\ll k\left|\frac{\partial}{\partial z}\phi_m\right|\ll k^2|\phi_m|.\tag{9}$$

With Eqs. (8) and (9), Eq. (6) yields

$$i\left[\frac{\partial}{\partial t}+\left(\frac{\hbar k}{m}\right)\frac{\partial}{\partial z}\right]\phi_{1f}=g_1(|\phi_{1f}|^2+2|\phi_{1b}|^2)\phi_{1f}+g_x[(|\phi_{2f}|^2+|\phi_{2b}|^2)\times\phi_{1f}+\phi_{2f}\phi_{2b}^\star\phi_{1b}] \quad (10)$$

and

$$i\left[\frac{\partial}{\partial t}-\left(\frac{\hbar k}{m}\right)\frac{\partial}{\partial z}\right]\phi_{1b}=g_2(|\phi_{1b}|^2+2|\phi_{1f}|^2)\phi_{1b}+g_x[(|\phi_{2b}|^2+|\phi_{2f}|^2)\times\phi_{1b}+\phi_{2b}\phi_{2f}^\star\phi_{1f}] \quad (11)$$

as well as two additional equations with $1\leftrightarrow 2$. In these equations we have scaled the nonlinear coupling constants to the overlap integral η and the total particle number N as

$$g_j\rightarrow\eta_j N g_j, \quad j=1,2,$$
$$g_x\rightarrow\eta_x N g_x. \quad (12)$$

The factors of 2 appearing in Eqs. (10) and (11) result from the nonlinear nonreciprocity familiar in nonlinear optics.

III. STEADY STATE

To find the steady state of the system, we proceed by first observing that the total atomic density

$$\varrho=|\phi_{1f}|^2+|\phi_{1b}|^2+|\phi_{2f}|^2+|\phi_{2b}|^2 \quad (13)$$

is a constant of motion. For simplicity we take $g_1=g_2=g_x\equiv g$ (this can be achieved by tuning the scattering lengths via, e.g., Feshbach resonance and/or by adjusting the transverse potential V_j); in the optical analog this corresponds to a purely electrostrictive Kerr medium. Dropping the time derivatives from Eqs. (10) and (11) and introducing the scaled velocity

$$v=\frac{\hbar k}{mg} \quad (14)$$

gives then

$$iv\frac{d\phi_{1f}}{dz}=\varrho\phi_{1f}+R\phi_{1b},$$
$$-iv\frac{d\phi_{1b}}{dz}=\varrho\phi_{1b}+R^\star\phi_{1f}, \quad (15)$$

and

$$iv\frac{d\phi_{2f}}{dz}=\varrho\phi_{2f}+R\phi_{2b},$$
$$-iv\frac{d\phi_{2b}}{dz}=\varrho\phi_{2b}+R^\star\phi_{2f}, \quad (16)$$

where the introduction of the new variable

$$R(z)\equiv\phi_{1f}\phi_{1b}^\star+\phi_{2f}\phi_{2b}^\star \quad (17)$$

allows us to decouple the evolution of the two internal components of the field for two condensate species 1 and 2. This can be seen from the observation that

$$\frac{dR}{dz}=\frac{d\phi_{1f}}{dz}\phi_{1b}^\star+\phi_{1f}\frac{d\phi_{1b}^\star}{dz}+\frac{d\phi_{2f}}{dz}\phi_{2b}^\star+\phi_{2f}\frac{d\phi_{2b}^\star}{dz}=-\frac{i}{v}3\varrho R, \quad (18)$$

which yields

$$R(z)=R_0e^{-i/v3\varrho z}. \quad (19)$$

We can therefore determine the steady state for the two internal states of the condensate separately.

Substituting the new rotating field amplitudes

$$\psi_{1f}=\phi_{1f}e^{i/v\,\varrho z},$$
$$\psi_{1b}=\phi_{1b}e^{-\frac{i}{v}\varrho z}, \quad (20)$$

into Eqs. (15) yields the second-order differential equation

$$\frac{d^2\psi_{1f}}{dz}=-\frac{i\varrho}{v}\frac{d\psi_{1f}}{dz}+\frac{|R_0|^2}{v^2}\psi_{1f}, \quad (21)$$

which shows that the propagation of ψ_{1f} is characterized by the spatial frequencies

$$k_\pm=-\frac{\varrho}{2v}\pm\frac{1}{2v}\sqrt{\varrho^2-4|R_0|^2}. \quad (22)$$

It can be shown that

$$M^2\equiv\varrho^2-4|R_0|^2\geqslant 0 \quad (23)$$

so that $\psi_{1f}(z)$ satisfies

$$\psi_{1f}(z)=e^{-(i\varrho/2v)z}\left[A_{1f}\sin\left(\frac{M}{2v}z\right)+B_{1f}\cos\left(\frac{M}{2v}z\right)\right], \quad (24)$$

the constants A_{1f} and B_{1f} being determined by the boundary conditions. We observe that A_{1f} depends on both $\psi_{1b}(0)$ and R_0, and hence on the boundary conditions for all four fields, $\phi_{1f}(0)$, $\phi_{1b}(L)$, $\phi_{2f}(0)$, and $\phi_{2b}(L)$. Therefore the equations of motion of all four fields need to be solved and used to calculate the respective coefficients for any one field. The explicit forms of the coefficients $A_{\mu i}$ and $B_{\mu i}$, where $\mu=1,2$ and $i=f,b$, are given in Appendix A.

Further analytical progress can be achieved by decomposing the field ψ_{1f} into a real amplitude and phase following Ref. [31],

$$\psi_{1f}=\sqrt{\rho_{1f}}\exp(i\vartheta_{1f}), \quad (25)$$

and concentrating on the field amplitudes only. One finds readily

$$\rho_{1f}(z)=\beta\pm\sqrt{|\alpha|^2-[\rho_{1f}(0)-\beta]^2}\sin\left(\frac{M}{v}z\right)+(\rho_{1f}(0)-\beta)\cos\left(\frac{M}{v}z\right), \tag{26}$$

where

$$\alpha=\frac{1}{2}(A_{1f}^2+B_{1f}^2),$$
$$\beta=\frac{1}{2}(|A_{1f}|^2+|B_{1f}|^2), \tag{27}$$

and the sign in front of the square root in Eq. (26) is determined by the sign of $A_{1f}B_{1f}^{\star}+A_{1f}^{\star}B_{1f}$. Similar relations hold for the other field components.

One advantage of concentrating on the amplitudes $\rho_{\mu i}$ only is that it is sufficient to know one of them to determine the others. This follows from the fact that

$$\frac{d\rho_{1f}}{dz}=\frac{d\rho_{1b}}{dz}=-\frac{d\rho_{2f}}{dz}=-\frac{d\rho_{2b}}{dz}, \tag{28}$$

which allows us to introduce the three conserved quantities

$$\rho_f\equiv\rho_{1f}(z)+\rho_{2f}(z),$$
$$\rho_b\equiv\rho_{1b}(z)+\rho_{2b}(z),$$
$$\rho_x\equiv\rho_{1f}(z)+\rho_{2b}(z), \tag{29}$$

so that

$$\rho_{1b}(z)=\rho_b-\rho_x+\rho_{1f}(z),$$
$$\rho_{2f}(z)=\rho_f-\rho_{1f}(z),$$
$$\rho_{2b}(z)=\rho_x-\rho_{1f}(z). \tag{30}$$

The existence of these conservation laws was previously pointed out in the context on nonlinear optics in Refs. [31] and [35].

For concreteness, we now consider the specific example where the intensities of the forward- and backward-propagating fields are equal,

$$\rho_f=\rho_b, \tag{31}$$

and

$$\rho_{1b}(L)=\rho_b=\varrho/2,$$
$$\rho_{2b}(L)=0. \tag{32}$$

Under these conditions, one finds readily that

$$|R_0|^2=\rho_b\rho_{1f}(L)=\frac{1}{2}\varrho\rho_{1f}(L) \tag{33}$$

and

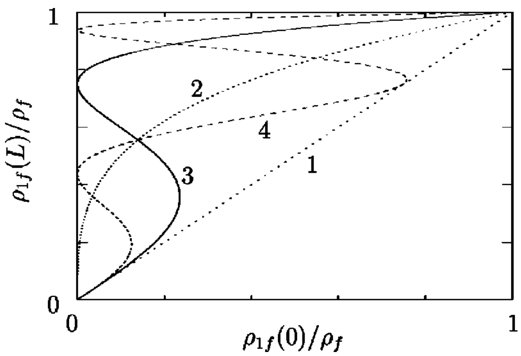

FIG. 2. Normalized output intensity $\rho_{1f}(L)$ versus normalized input intensity $\rho_{1f}(0)$ from Eq. (35). Curve (1) $L/L_c=0$, Curve (2) $L/L_c=2\pi$, Curve (3) $L/L_c=4\pi$, and Curve (4) $L/L_c=8\pi$, with L_c as defined in Eq. (39).

$$|\alpha|=\beta=\rho_{1f}(L)/2. \tag{34}$$

With Eqs. (33) and (34), Eq. (26) reduces to the remarkably simple form

$$\frac{\rho_{1f}(0)}{\rho_{1f}(L)}=\cos^2(\kappa L/2), \tag{35}$$

where

$$\kappa=M/v=\left(\frac{2mg}{\hbar k}\right)\varrho\sqrt{1/4-\rho_{1f}(L)/2\varrho}. \tag{36}$$

$1/\kappa$ defines a characteristic length. Equation (35) predicts a multivalued relationship between the input and output intensities ρ_{1f}. The longer the κ, the higher the order of ‘‘multistability’’ predicted by Eq. (35). Fig. 2 illustrates the input-output relationship of ρ_{1f}.

Alternatively, and recalling Eqs. (12) and (14) we observe that the argument $\kappa L/2$ of the cosine function in Eq. (35) is also proportional to the total density of atoms. This leads us to expect some interesting behavior when varying the number of particles involved, a scheme whose optical analog has been the object of considerable work [31,33–35]. However, we do not further investigate these questions in the present paper, which is limited to the case of fixed total atomic density.

Returning from the scaled version (12) of the coupling constant g to its original definition (2) via Eqs. (7), we observe that for a transversely homogeneous sample, the factor $g\varrho$ in Eq. (36) becomes $g\varrho_V$, where ϱ_V is the volumetric density of the atomic system (as opposed to its linear density ϱ). Eq. (36) becomes then

$$\kappa=k\left(\frac{2m}{\hbar^2k^2}\right)\hbar g\varrho_V\sqrt{1/4-2\rho_{1f}(L)/2\varrho}$$
$$=k\left(\frac{E_{mf}}{E_{ke}}\right)\sqrt{1/4-\rho_{1f}(L)/2\varrho}, \tag{37}$$

where we have introduced the kinetic energy $E_{ke}=\hbar^2k^2/2m$ and the mean-field energy $E_{mf}=\hbar g\varrho_V$.

Introducing the healing length

$$l_h = \sqrt{\frac{\hbar}{2mg\varrho_V}} \tag{38}$$

and the de Broglie wavelength $\lambda_{db} = 2\pi/k$ shows that the multistable properties of the system are fully determined by the characteristic length

$$L_c = \frac{E_{ke}}{kE_{mf}} = 4\pi^2 \frac{l_h^2}{\lambda_{db}}. \tag{39}$$

IV. STABILITY ANALYSIS

In this section, we analyze the stability of the steady-state solution (35) against small classical perturbations. For simplicity, we assume that the fields at the boundaries of the interaction region are real,

$$\phi_{1f}(0) = \sqrt{\rho_{1f}},$$

$$\phi_{2f}(0) = \sqrt{\rho_f - \rho_{1f}},$$

$$\phi_{1b}(L) = 0,$$

$$\phi_{2b}(L) = \sqrt{\rho_b}. \tag{40}$$

The first approach proceeds by expressing the condensate wave function $\phi_{1f}(z,t)$ and its complex conjugate as

$$\phi_{1f}(z,t) = \phi_{1f_{ss}}(z,t) + \delta_{1f}(z) e^{-i\lambda t},$$

$$\phi_{1f}^\star(z,t) = \phi_{1f_{ss}}^\star(z,t) + \epsilon_{1f}(z) e^{-i\lambda t}, \tag{41}$$

and linearizing the equations of motion (10) and (11), and similarly for the other field components. The spectrum of eigenvalues λ can be found by discretizing the resulting system of equations with N points along the z axis, which yields a sparse $8N \times 8N$ eigenvalue problem that can be solved numerically using standard techniques. The steady-state solution is then unstable only if eigenvalues with positive imaginary parts appear in the spectrum.

In addition to this temporal stability, we have also carried out a full spatio-temporal analysis by solving directly the linearized form of Eqs. (10) and (11) for small perturbations about the steady state of the fields.

Both approaches indicate that the only stable branch of the solution (35) is the ''uppermost branch,'' i.e., the branch corresponding to the highest $\rho_{1f}(L)$ for a given $\rho_{1f}(0)$ that corresponds to the condition

$$0 \leq \frac{\kappa L}{2} < \pi/2. \tag{42}$$

Figure 3 shows a typical result for the temporal evolution of δ_{1f} at $z = L$ in both an unstable and a stable branch. After some short-time transients, the unstable dynamics becomes completely dominated by the largest positive eigenvalue and the growth of the small perturbation becomes exponential.

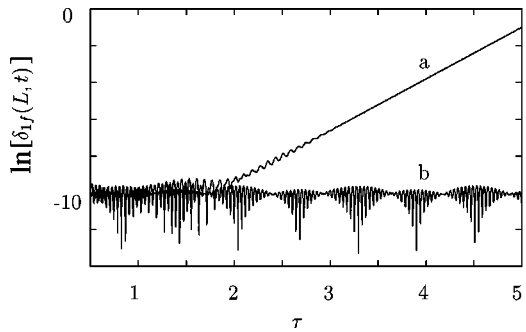

FIG. 3. $\ln[\delta_{1f}(L,\tau)]$ for $\rho_{1f_{ss}}(L) = 0.2\rho_f$. $\delta_{1f}(L,\tau)$ is scaled to the intensity ρ_f of the forward moving field and the time τ is in units of the round-trip time through the interaction region. Curve (a) is an example of unstable behavior at $L/L_c = 4\pi$ ($\kappa L/2 \approx 0.89\pi$), while curve (b) shows stability at $L/L_c = 1.6\pi$ ($\kappa L/2 \approx 0.36\pi$).

V. SELF-OSCILLATIONS

An important consequence of the stability analysis is the prediction of a self-oscillation threshold in the system, as can be seen by considering the case $\rho_{1f}(0) = 0$, that is, no input field in mode ''$1f$.'' In that case, Eq. (35) reduces to

$$\rho_{1f}(L)\cos^2(\kappa L/2) = 0. \tag{43}$$

Hence in the stable region given by Eq. (42), $\rho_{1f}(L)$ must be 0; while in the unstable region, $\rho_{1f}(L)$ may take finite values, which results from the amplification of fluctuations. The onset of instability is given by

$$\kappa L = kL \left(\frac{E_{mf}}{E_{ke}} \right) \sqrt{1/4 - \rho_{1f}(L)/2\varrho} = \pi. \tag{44}$$

Since the argument of the square root is always less than 1/4, we have that

$$\kappa L \leq \frac{kL}{2} \left(\frac{E_{mf}}{E_{ke}} \right). \tag{45}$$

Hence the threshold condition (44) cannot be met unless

$$\left(\frac{E_{mf}}{E_{ke}} \right) \geq \frac{2\pi}{kL}, \tag{46}$$

or

$$\frac{l_h^2}{L\lambda_{db}} \leq \frac{1}{8\pi^3}, \tag{47}$$

which can be recast as

$$\frac{L}{L_c} \geq 2\pi. \tag{48}$$

If this threshold condition is satisfied, the field ϕ_{1f} undergoes a second-order-like phase transition to self-oscillations, as illustrated in Fig. 4.

The physical origin of the self-oscillations is the distributed feedback resulting from the cross-phase modulation

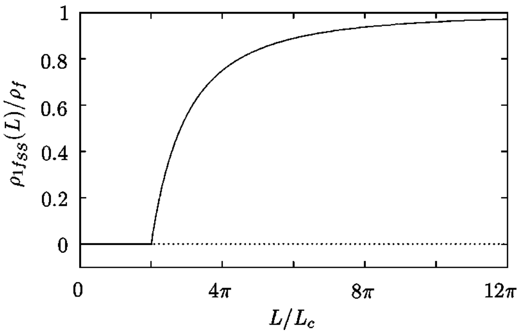

FIG. 4. Self-oscillation threshold of the intensity $\rho_{1f}(L)$, normalized to ρ_f, as a function of the interaction length L. Above threshold, this field spontaneously builds up from fluctuations even in the absence of input, $\rho_{1f}(0)=0$.

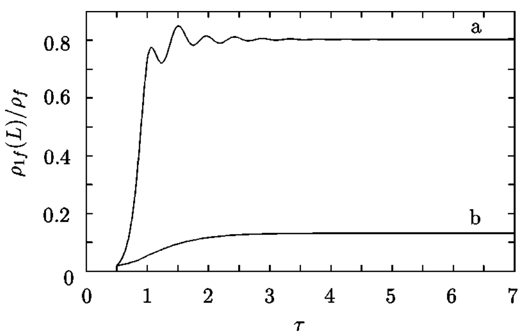

FIG. 5. $\rho_{1f}(L,\tau)$, normalized to ρ_f, for $\rho_{1f}(0)=0.01\varrho$. The time is in units of the round-trip time through the interaction medium. Curve (a) is in the regime with only one high-output stable branch at $L/L_c=4\pi$; curve (b) is at $L/L_c=1.6\pi$ where for every (low) output intensity there exists a stable steady-state field configuration.

with the other fields present. In order to lead to gain at the wavelength of ϕ_{1f}, this grating must itself be modulated with period $2\pi/k$. But the mean-field energy of the condensate fights against the creation of such spatial modulation. The healing length, whose associated momentum l_h^{-1} yields a kinetic-energy contribution equal to the mean-field energy, is the smallest length scale over which the required changes can occur. Hence, it is not surprising that the threshold condition should be related to the healing length, the length of the sample, and the atomic de Broglie wavelength.

It is interesting to note that the quantity $l_h^2/\lambda_{db}L$ is reminiscent of the Fresnel number $\mathcal{F}=a^2/\lambda L$ in optics, where a is the aperture of the system, λ the wavelength, and L the distance of propagation. The Fresnel number is a measure of the number of transverse modes that can be excited in an optical system. For very large Fresnel numbers, the wave can well be approximated as a plane wave, while diffraction effects and multiple transverse modes become important for small $\mathcal{F}$. The present situation is different in that we now consider the longitudinal stability of the system. Still, the analogy is rather telling. For samples of length short or comparable to the healing length, the condensate is so stiff as to prevent the generation of higher-longitudinal modes, hence the instability requires a condensate much larger than l_h. As such, $l_h^2/\lambda_{db}L$ can be thought of as the *longitudinal Fresnel number* of the condensate, with the healing length playing a role similar to that of the system aperture a in optics.

The onset of self-oscillations is illustrated in Fig. 5, which shows the evolution of $\rho_{1f}(L,t)$ for $\rho_{1f}(0,t)=0.01\varrho/2$, this small value simulating some small fluctuation about $\rho_{1f}(0,t)=0$. This simulation assume that all field amplitudes inside the interaction region $(0<z\leqslant L)$ are initially equal to zero.

VI. SUMMARY AND CONCLUSION

In summary, we have studied a system of counterpropagating two-component Bose-Einstein condensates in a waveguide configuration. This system exhibits interesting nonlinear behavior such as four-wave mixing and self-oscillations. We have presented an analytical solution of the steady-state field equations and found a multivalued relationship between the input and the output field intensities. Through a linear perturbation analysis as well as a full numerical study, we have found that one and only one branch of solutions is stable for a given input configuration. The onset of the instability depends on a parameter in close analogy with the Fresnel number in optics.

We remark that these results were obtained under the assumption that all the effective scattering lengths are the same $(g_1=g_2=g_x)$. In future work, we plan to investigate the case of unequal scattering lengths, which will make our system formally equivalent to the case of counterpropagating light fields in a nonelectrostrictive Kerr medium. The analogy with the optical system also suggests that it would be desirable to allow for different intensities of the two counterpropagating matter-wave fields. It has been shown that bi- or multistable solutions exist in these nonlinear optical systems. It will be interesting to see if such a matter-wave system can also exhibit multistability.

Finally, it will be worthwhile to extend the analysis past the Hartree mean-field theory in order to study the onset of nonclassical effects, such as the squeezing associated with the anomalous density of the system.

The experimental realization of this system is certainly challenging, but we see no fundamental problems using present day technology. Indeed, the question of stability in wave-mixing processes will most likely arise naturally in the next generation of atom interferometry experiments.

ACKNOWLEDGMENTS

This work was supported in part by Office of Naval Research Contract No. 14-91-J1205, National Science Foundation Grant PHY98-01099, the Army Research Office, and the Joint Services Optics Program. J.H. gratefully acknowledges support by the ''Konrad Adenauer Stiftung.''

APPENDIX A

Solving Eq. (21) and its counterpart for the backward moving field and inserting the results into Eqs. (20) gives

$$\phi_{1f}(z)=e^{-i(3\varrho/2v)z}\left[A_{1f}\sin\left(\frac{M}{2v}z\right)+B_{1f}\cos\left(\frac{M}{2v}z\right)\right],$$

$$\phi_{1b}(z)=e^{i(3\varrho/2v)z}\left[A_{1b}\sin\left(\frac{M}{2v}z\right)+B_{1b}\cos\left(\frac{M}{2v}z\right)\right], \tag{A1}$$

and similarly for $1\leftrightarrow 2$. The boundary conditions are $\phi_{1f}(0)$, $\phi_{1b}(L)$, $\phi_{2f}(0)$, and $\phi_{2b}(L)$. Since the four fields are coupled by $R_0=B_{1f}B_{1b}^{\star}+B_{2f}B_{2b}^{\star}$ it is necessary to consider all fields to determine the coefficients $A_{\mu i}$ and $B_{\mu i}$. We start from Eqs. (A1), and derive expressions for $\phi_{jf}(0)$, $d\phi_{jf}(0)/dz$, $\phi_{jb}(L)$, and $d\phi_{jb}(0)/dz$, $j=1,2$ in terms of these coefficients and use the relations (10) to close this set of equations.

For $\sin(ML/2v), \phi_{1f}(0)$, and $\phi_{2f}(0)\neq 0$ we find

$$B_{1f}=\phi_{1f}(0),$$

$$B_{2f}=\phi_{2f}(0),$$

$$B_{1b}=-\frac{e^{-3i\varrho L/2v}M(\phi_{1b}(L)+\phi_{2b}(L)/g(|B_{2f}|^2))}{\sin(ML/2v)[g(|B_{1f}|^2)+4|B_{1f}|^2|B_{2f}|^2/g(|B_{2f}|^2)]},$$

$$B_{2b}=\frac{i2B_{1f}^{\star}B_{1b}B_{2f}-e^{-3i\varrho L/2v}M\phi_{2b}(L)/\sin(ML/2v)}{g(|B_{2f}|^2)},$$

$$A_{1b}=\frac{\phi_{1b}(L)e^{-3i\varrho L/2v}-B_{1b}\cos((M/2v)L)}{\sin((M/2v)L)},$$

$$A_{2b}=-B_{2b}/\tan(ML/2v),$$

$$A_{1f}=\frac{i}{M}[\varrho B_{1f}-2(B_{1f}B_{1b}^{\star}+B_{2f}B_{2b}^{\star})B_{1b}],$$

$$A_{2f}=\frac{i}{M}[\varrho B_{2f}-2(B_{1f}B_{1b}^{\star}+B_{2f}B_{2b}^{\star})B_{2b}], \tag{A2}$$

where

$$g(x)=i(\varrho-2x)-M/\tan(ML/2v). \tag{A3}$$

These equations simplify considerably in the specific case $\phi_{2b}(L)=0$ that we have analyzed in detail. Similar, but simpler equations are easily derived if one of the input fields is equal to zero or for $\sin(ML/2v)\neq 0$.

[1] J. Reichel, W. Hänsel, and T.W. Hänsch, Phys. Rev. Lett. **83**, 3398 (1999).
[2] D. Müller *et al.*, Phys. Rev. Lett. **83**, 5194 (1999).
[3] N.H. Dekker *et al.*, Phys. Rev. Lett. **84**, 1124 (2000).
[4] R. Folman *et al.*, Phys. Rev. Lett. **84**, 4749 (2000).
[5] E.A. Hinds and I.G. Hughes, J. Phys. D **32**, R119 (1999).
[6] M. Key *et al.*, Phys. Rev. Lett. **84**, 1371 (2000).
[7] E.A. Hinds and C. Eberlein, Phys. Rev. A **61**, 031404 (2000).
[8] M.-O. Mewes *et al.*, Phys. Rev. Lett. **78**, 582 (1997).
[9] B.P. Anderson and M.A. Kasevich, Science **282**, 1686 (1998).
[10] E.W. Hagley *et al.*, Science **283**, 1706 (1999).
[11] I. Bloch, T.W. Hänsch, and T. Esslinger, Phys. Rev. Lett. **82**, 3008 (1999).
[12] E. Goldstein, K. Plättner, and P. Meystre, Quantum Semiclassic. Opt. **7**, 743 (1995).
[13] E.V. Goldstein, K. Plättner, and P. Meystre, J. Res. Natl. Inst. Stand. Technol. **101**, 583 (1996).
[14] E.V. Goldstein and P. Meystre, Phys. Rev. A **59**, 1509 (1999).
[15] M. Trippenbach, Y. Band, and P.S. Julienne, Opt. Express **3**, 530 (1998).
[16] L. Deng *et al.*, Nature (London) **398**, 218 (1999).
[17] M. Trippenbach, Y.B. Band, and P.S. Julienne, Phys. Rev. A **62**, 023608 (2000).
[18] Y. Wu *et al.*, Phys. Rev. A **61**, 043604 (2000).
[19] G. Lenz, P. Meystre, and E.M. Wright, Phys. Rev. Lett. **71**, 3271 (1993).
[20] Weiping Zhang, D.F. Walls, and B.C. Sanders, Phys. Rev. Lett. **72**, 60 (1994).
[21] Weiping Zhang and D.F. Walls, Phys. Rev. A **49**, 3799 (1994).
[22] G. Lenz, P. Meystre, and E. M. Wright, Phys. Rev. A **50**, 1681 (1994).
[23] R. Dum, J.I. Cirac, M. Lewenstein, and P. Zoller, Phys. Rev. Lett. **80**, 2972 (1998).
[24] S. Burger *et al.*, Phys. Rev. Lett. **83**, 5198 (1999).
[25] J. Denschlag *et al.*, Science **287**, 97 (2000).
[26] M.H. Anderson *et al.*, Science **269**, 198 (1995).
[27] K.B. Davis *et al.*, Phys. Rev. Lett. **75**, 3969 (1995).
[28] C.C. Bradley, C.A. Sackett, J.J. Tollett, and R.G. Hulet, Phys. Rev. Lett. **75**, 1687 (1995).
[29] H.G. Winful and J.H. Marburger, Appl. Phys. Lett. **36**, 613 (1980).
[30] Y. Silberberg and I. Bar-Joseph, Phys. Rev. Lett. **48**, 1541 (1982).
[31] A.E. Kaplan and C.T. Law, IEEE J. Quantum Electron. **QE-21**, 1529 (1985).
[32] A.E. Kaplan, Opt. Lett. **8**, 560 (1983).
[33] J. Yumoto and K. Otsuka, Phys. Rev. Lett. **54**, 1806 (1985).
[34] G. Gregori and S. Wabnitz, Phys. Rev. Lett. **56**, 600 (1986).
[35] M.V. Tratnik and J.E. Sipe, Phys. Rev. A **35**, 2976 (1987).
[36] A.L. Gaeta, R.W. Boyd, J.R. Ackerhalt, and P.W. Milonni, Phys. Rev. Lett. **58**, 2432 (1987).
[37] D.N. Christodoulides, Phys. Rev. A **45**, 6605 (1992).
[38] D.J. Gauthier, M.S. Malcuit, and R.W. Boyd, Phys. Rev. Lett. **61**, 1827 (1988).
[39] D.J. Gauthier, M.S. Malcuit, A.L. Gaetha, and R.W. Boyd, Phys. Rev. Lett. **64**, 1721 (1990).
[40] C.K. Law, H. Pu, and N.P. Bigelow, Phys. Rev. Lett. **81**, 5257 (1998).
[41] E.V. Goldstein and P. Meystre, Phys. Rev. A **59**, 3896 (1999).
[42] Z.-B. Chen, Mod. Phys. Lett. B **14**, 31 (2000).